Wall Slip of Soft-Jammed Systems: A Generic Simple Shear Process

X. Zhang,[1] E. Lorenceau,[2] P. Basset,[3] T. Bourouina,[3] F. Rouyer,[1] J. Goyon,[1] and P. Coussot[1]
[1]*Université Paris-Est, Laboratoire Navier (ENPC-IFSTTAR-CNRS), 2 Allée Kepler, 77420 Champs sur Marne, France*
[2]*Université Grenoble-Alpes, CNRS, LIPhy, 38000 Grenoble, France*
[3]*Université Paris-Est, ESYCOM EA 2552, ESIEE Paris-CNAM-UPEM, 5 Boulevard Descartes, 77420 Champs sur Marne, France*
(Received 25 April 2017; revised manuscript received 5 October 2017)

From well-controlled long creep tests, we show that the residual apparent yield stress observed with soft-jammed systems along smooth surfaces is an artifact due to edge effects. By removing these effects, we can determine the stress solely associated with steady-state wall slip below the material yield stress. This stress is found to vary linearly with the slip velocity for a wide range of materials whatever the structure, the interaction types between the elements and with the wall, and the concentration. Thus, wall slip results from the laminar flow of some given free liquid volume remaining between the (rough) jammed structure formed by the elements and the smooth wall. This phenomenon may be described by the simple shear flow in a Newtonian liquid layer of uniform thickness. For various systems, this equivalent thickness varies in a narrow range (35 ± 15 nm).

DOI:

Various materials, such as foams, emulsions, concentrated suspensions, and colloids, are soft-jammed systems; i.e., they can flow only when submitted to a stress larger than a yield stress (τ_c); otherwise, they behave as solids [1]. In many situations, it is observed that such materials glide along smooth solid surfaces, in the sense that the bulk material apparently moves as a rigid block for a stress lower than τ_c [2–4]. This effect is called wall slip. Its impact on flow characteristics is dramatic, since it may make such materials, otherwise at rest, flow at a high velocity under small stresses. Thus, wall slip can overturn the standard continuum mechanics description assuming adherence. This modification of the interaction with the walls can be used to facilitate the transport of products such as in food digestion [5], cosmetic sensory perception [6], coal water slurry in pipes [7], fresh concrete pumping over a long distance [8], removal of food debris, and microbial films [9].

Even if it has for a long time been admitted that it results from the formation of a layer with different components than in the bulk [2], the physics of wall slip is still poorly advanced. Note that this effect must not be confused with shear-banding [10] or confinement effects [11] in jammed systems, which occur beyond the yield stress. Here we focus on flow characteristics below τ_c, so that such effects are *a priori* negligible.

To gain a quantitative measurement and understanding concerning wall slip, the basic approach consisted of fitting a model to the apparent flow curve (shear stress vs velocity) in the slip regime (i.e., for a stress below the yield stress), or directly measuring the slip velocity, and possibly discussing the physical origin of the parameters, for the different material classes (concentrated suspensions [12–15], soft particle suspensions [16,17], emulsions [18–20], and foams [20–22]). Generally, power-law dependencies for the stress vs slip velocity variations were obtained, with an exponent ranging from ½ to 1. An advanced physical explanation [16] assumes that the liquid layer thickness varies with the balance between attractive (due to osmotic pressure resulting from the jammed nature of the system) and repulsive forces (due to lubricating viscous forces). Some similar approaches were developed independently for individual bubbles or bubble film [23] with later further sophistication [24]. In particular, for foams, linear and nonlinear regimes were suggested to occur depending on the relative values of colloidal interaction and viscous effects [25]. On the other side, for hard-sphere colloidal suspensions, it was shown [13–15] that a linear velocity variation plus a constant (residual) yield stress term well represents their data, but the liquid thickness associated to the linear term was shown to be independent of the osmotic pressure. Such a residual yield stress was observed in most studies, but it appears somewhat contradictory with the existence of a liquid layer allowing wall slip, and a detailed analysis of wall-element interactions could not identify a clear origin for this effect [13,18].

Here, by determining precisely the stress vs velocity law from sufficiently long creep tests, we can show that the residual yield stress is due to edge effects (evaporation along the line of contact), and, after its removal, a linear stress vs velocity law is found whatever the type of interactions between the suspended elements, their concentration, and the interactions with the solid surface.

A simple observation provides a straightforward view and analysis of the main characteristics of wall slip: A small volume of a yield stress fluid (an oil-in-water emulsion) placed over an inclined smooth surface slowly moves

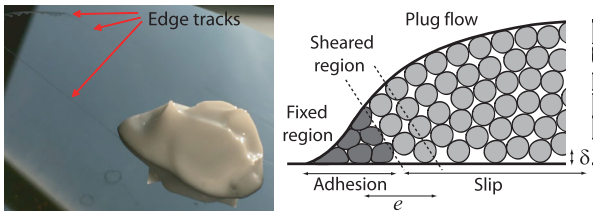

F1:1 FIG. 1. (a) View of a heap of emulsion after some motion (from
F1:2 the top left) on a smooth inclined surface. (b) Schematic aspect of
F1:3 the sample cross section close to the contact line showing the
F1:4 different flow regions and their microstructural origin (suspended
F1:5 elements in dark or light gray, interstitial liquid in white).

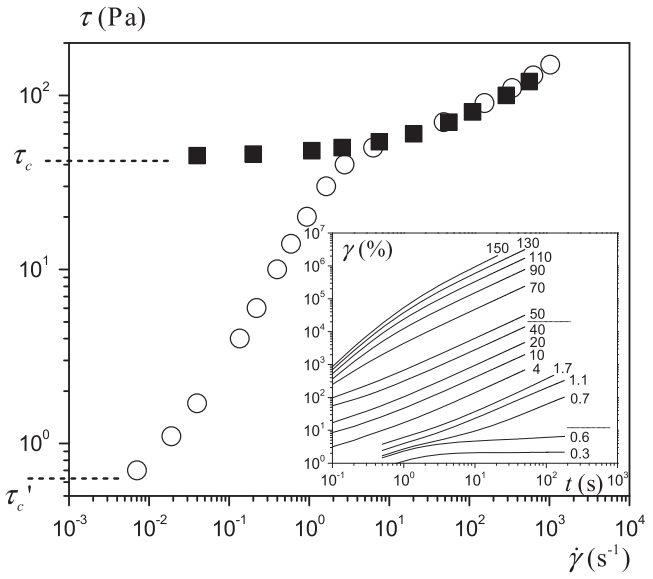

F2:1 FIG. 2. Direct concentrated emulsion (82%): flow curve (with
F2:2 rough surfaces) (solid squares) and apparent flow curve in the
F2:3 presence of wall slip along one smooth surface (open circles).
F2:4 The inset shows creep test data for the latter case. The numbers
F2:5 correspond to stress values in Pascals. The dotted lines mark the
F2:6 transition to slip (lower line) and the bulk yielding (upper line).

downwards as a rigid block [see Fig. 1(a)]. A detailed observation of the traces left on the surface reveals (i) apparent thick tracks of material along the edges of the sample which persist over time and (ii) a transient thin liquid layer which soon fully evaporates behind the sample, suggesting that the material is sheared only in an interstitial liquid layer along the wall.

In order to get precise information on the wall slip of such a material, we follow a procedure which allows us to clearly identify the rheological characteristics of simple or thixotropic [26] yield stress fluids. This consists of applying a shear stress (τ) to the material and following its apparent deformation (γ) in time (t). Here we use a rheometer equipped with parallel plates with one rough surface and one smooth surface (i.e., of roughness much smaller than the element size; see [27]), separated by a distance (i.e., gap) h. τ and γ are computed from the torque and rotation velocity, through expressions corresponding approximately to the local values at ¾ of the distance from the axis for a Newtonian or a yield stress fluid [27]. The test is then repeated at another stress level, with the material prepared in the same initial state (preshear and then short rest). Under such conditions, the overall results are reproducible and do not depend on the order of the tests at different stress values.

First we focus on a concentrated emulsion (see [27]), in which the element interactions are essentially repulsive. We observe two distinct regimes (see the inset in Fig. 2): For τ smaller than a critical value (τ_c'), the material is just slightly deformed over a short time, and then γ reaches a plateau, indicating that no more motion occurs; for stresses larger than τ_c', after a short period γ increases linearly with time, indicating that the material flows steadily. In that case, we can define $\dot{\gamma}$, the apparent steady-state shear rate associated to τ, as the slope of the $\gamma(t)$ curve. The same experiment with two rough surfaces provides two similar regimes but with a transition now observed at a critical stress equal to τ_c, the yield stress of the material above which the material flows in bulk, with $\tau_c' < \tau_c$. We deduce that, for $\tau_c' < \tau < \tau_c$, the material may flow only in a thin (slip) layer along the smooth wall, in agreement with the observations in Fig. 1. This is confirmed by the observation that a vertical mark at the sample periphery moves as a rigid block attached to the rough plate. Moreover, tests with different gaps for the same stress give an apparent shear rate increasing with the inverse of the gap, which means that the flow characteristics in this layer depend only on τ. We can then define the slip velocity ($V_S = \dot{\gamma} h$) as the relative velocity between this block and the smooth wall.

It is now possible to represent the apparent flow curve of the material, i.e., τ vs $\dot{\gamma}$, which appears to be made of two parts (see Fig. 2): Below τ_c, τ strongly increases with $\dot{\gamma}$; beyond τ_c, the curve flattens and soon joins the effective flow curve of the bulk material (obtained with rough surfaces), indicating that slip can still occur but becomes negligible with regards to the flow rate induced by the bulk flow, when τ increases. We thus get the standard aspect of apparent flow curves with smooth surfaces, as observed with a variety of simple yield stress fluids for which, as for our materials, repulsive interactions between suspended elements dominate [12–15,18–22].

Let us now focus on materials in which suspended element interactions are essentially attractive (i.e., weak flocculation) (see [27]). In general, such materials exhibit significant thixotropy, due to their relatively long time of restructuring. Our rheometrical protocol with rough surfaces allows us to get the typical flow curve [10] similar to that of a simple yield stress fluid, except that no (homogeneous) steady-state flow may be obtained below a critical shear rate $\dot{\gamma}_c$ (see Fig. 3). During creep tests, there is a viscosity bifurcation [28]: The material first significantly flows (it undergoes very large deformation) and finally

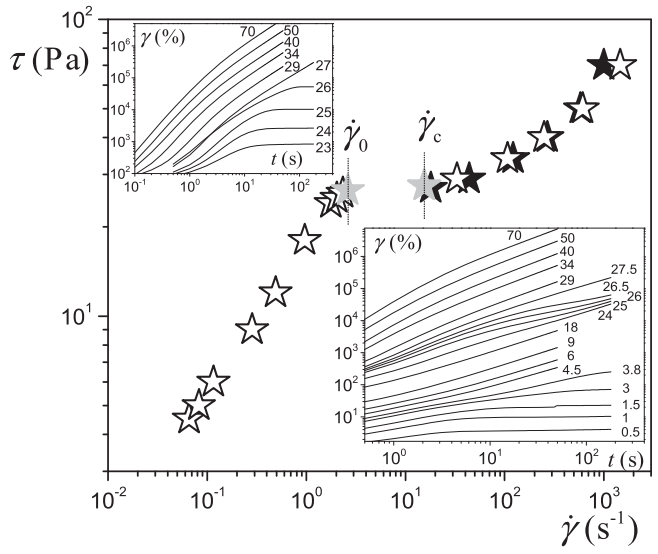

FIG. 3. Flow curve of a thixotropic clay-water suspension for fully rough (solid stars) and partially smooth (open stars) surface conditions. The insets show creep curves for rough (top) and smooth (bottom) surfaces. The data shown as gray stars (for 27 Pa) correspond to the jump in the apparent steady state observed for a stress between 24 and 27.5 Pa (see the bottom inset).

evolves either towards stoppage ($\dot{\gamma} = 0$) or to $\dot{\gamma} > \dot{\gamma}_c$ around τ_c (see the top inset in Fig. 3).

For such a material, with a smooth surface, a steady wall slip occurs for $\tau < \tau_c$. Increasing τ leads to increasing V_S, and when $\tau > \tau_c$ the wall slip tends to become negligible. Remarkably, we expect that if $\dot{\gamma}_c$, which depends on the bulk material properties, is larger than the shear rate at the intersection ($\dot{\gamma}_0$) of the effective (bulk) flow curve and the wall slip flow curve, there will be a range of $\dot{\gamma}$ in which the material cannot flow steadily if the stress is imposed: The material evolves towards bulk solidification with wall slip leading to $\dot{\gamma} \approx \dot{\gamma}_0$, if $\tau = \tau_c(1-\varepsilon)$ (with $\varepsilon \ll 1$); it flows and undergoes a significant viscosity decrease so that wall slip is apparently negligible, if $\tau = \tau_c(1+\varepsilon)$. This prediction is in agreement with the evolution of the experimental creep curves around τ_c, here equal to 27.5 Pa (see the bottom inset in Fig. 3), so that, finally, in the flow curve, there is effectively a jump (by about one decade) between the maximum shear rate for pure slip flow ($\dot{\gamma}_0$) and the minimum shear rate associating slip and bulk flow ($\dot{\gamma}_c$) (see Fig. 3). If, on the contrary, $\dot{\gamma}_c < \dot{\gamma}_0$, there is no such jump, as for simple yield stress fluids. Thus, despite a strong change of the structure characteristics, there is apparently no significant change in the slip characteristics. The only possible difference is situated at the transition from the slip and the shear regime, due to material thixotropy.

With our procedure consisting of waiting a sufficient time to reach a clear steady-state flow, we can rather precisely identify τ_c'. For example, for the material in Fig. 2, we can conclude that τ_c' is situated between 0.6 and 0.7 Pa. τ_c' has so far been considered as reflecting some attractive interaction between the suspended elements and the solid surface [29]. However, the reproducibility of our measurements in the slip regime, with an uncertainty of the order of 2% on the apparent flow curve data, is excellent, except at the approach of τ_c', where the uncertainty becomes of the order of 20% (see Fig. 4). An even more critical observation is that τ_c' significantly increases when the sample diameter is decreased while keeping h constant (see Fig. 4). In such a case, the flow conditions along most of the wall surface are *a priori* identical, but if some edge effect induces an additional stress (τ_a) acting over a constant width (e) along the sample periphery, it will induce an additional component in the apparent stress, proportional to the inverse of the sample radius, i.e., $\tau \approx \tau_0 + 3e\tau_a/R$ (see [27] for a detailed analysis). This roughly corresponds to the observed trend (see the inset in Fig. 4).

Our assumption is supported by the observation of a track stuck on the plane surface along the line of contact of the heap after its displacement [see Fig. 1(a)]. This means that there is some flow of the material in a thin (bulk) volume along the contact line [see Fig. 1(b)]. A similar flow certainly occurs at the sample periphery in a rheometrical

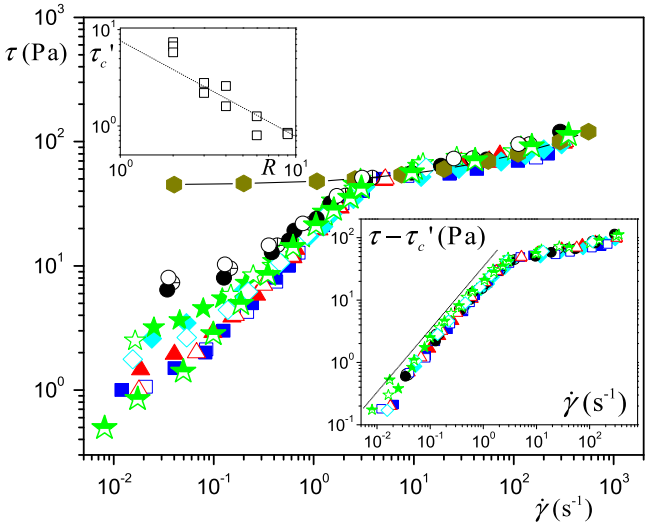

FIG. 4. Apparent flow curves of an emulsion (82%) for the same gap and different plate diameters: 9 cm (squares), 6 cm (triangles), 4 cm (diamonds), 3 cm (stars), 3 cm with oil film at the sample periphery (half-filled stars), and 2 cm (circles). Hexagons show data with two rough plate surfaces. Several tests carried out by changing the sample while keeping the same surface are shown for each diameter in order to appreciate the reproducibility. Note that, in order to remove the impact of the sample shape at the periphery, which increases when sample R decreases, τ has been rescaled by a factor of around 1 to get the same stress values for $\dot{\gamma}_0$ (see [24]). The bottom inset shows the stress minus the residual yield stress vs shear rate. The dotted line of slope 1 is a guide for the eye. The top inset shows τ_c' (in Pascals) values as a function of R (in centimeters).

test, which requires one to apply a stress larger than τ_c in a thin region located near the periphery, and leads to an apparent stress likely increasing with the local shear rate but tending to τ_c' at low $\dot{\gamma}$. The origin of this effect might be that some suspended elements tend to be attached to the solid surface at the contact line [see Fig. 1(b)], as a result of a slight evaporation effect at the contact line [30]. This statement is confirmed by a simple test: If we significantly limit the evaporation by coating the sample periphery with a thin oil film just after its setup on the bottom plane, the apparent τ_c' effect almost disappears (see Fig. 4). The basic ingredients required to see this effect, which are the existence of a contact line, suspended elements, and evaporation, are present in most of the experimental situations.

Under these conditions, it is crucial to remove the stress associated with edge effects from the apparent stress. As a first approximation, this may be done by withdrawing τ_c' from τ, thus neglecting some possible slight increase of the edge effect stress with $\dot{\gamma}$. In that case, all the data for different sample diameters fall along a master curve (see the inset in Fig. 4), which means that we have obtained a consistent apparent flow curve in the slip regime whatever the sample dimension, and this flow curve is strictly associated with the wall slip effect.

Therefore, we can focus on these intrinsic wall slip properties by looking at the variation of V_S as a function of the shear stress strictly associated with wall slip $\tau_S = \tau - \tau_c'$, i.e., in the absence of edge effects. We find that V_S essentially follows a straight line of slope 1, over the whole range of τ_S (see Figs. 4 and 5). Note that our procedure for the determination of τ_c' allows us to avoid any significant ambiguity about the observed slope of variation (i.e., 1), whereas the use of an arbitrary lower value for τ_c' may, particularly when τ_c' is not much smaller than τ_c, wrongly lead one to conclude that $V_S \propto \tau_S^p$ with p distinctly larger than 1. In order to compare the different data relatively to the regime change observed for $\tau_S = \tau_c$, V_S and τ_S must be rescaled by τ_c. This makes it possible to observe (see Fig. 5) a general tendency to a slope slightly larger than 1 at the approach of the regime change, say, in the range $[\tau_c/2; \tau_c]$, which might reflect a tendency to lubricational repulsion as expected from models [16,18,23].

In addition, V_S is inversely proportional to the interstitial liquid viscosity (μ) for emulsions with the same concentration and droplet size (see Fig. 5). This finally means that a general wall slip law, $\tau_S = \mu V_S/\delta$ for $\tau < \tau_c$, well represents the data in a three-decade range of τ_S/τ_c, with δ a material parameter.

Such results are apparently consistent with the existence of a uniform layer of thickness δ of a Newtonian liquid solution sheared along the wall while the bulk moves as a solid. Remarkably, assuming this solution essentially corresponds to the interstitial liquid, δ appears to be situated in

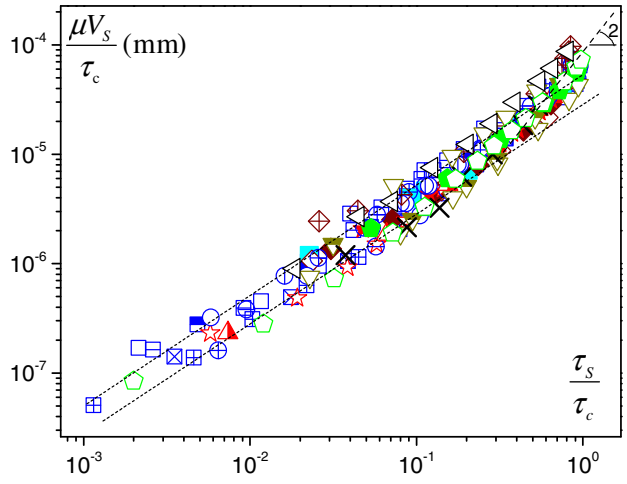

FIG. 5. Wall slip velocity for various materials (see [27] for detailed data) as a function of slip stress: emulsions at different concentrations on silicon surface (blue squares), emulsions with different surfactants and solid surfaces (blue circles), emulsion with a water-glycerol solution (with a viscosity 15 times that of water) as interstitial liquid (light blue solid square), bentonite suspensions at different concentrations (brown diamonds), inverse emulsions (dark yellow inverse triangles) (here using 1.5 μ; see [27]), Carbopol gels (green pentagons), ketchup (red solid stars), mustard (red open stars), foam (crosses), and direct emulsion (82%) over a Teflon surface (black cones). The dashed lines correspond to the equation $\tau_S = \mu V_S/\delta$ with $\delta = 30$ nm and $\delta = 50$ nm.

a narrow range, say, 20–50 nm (see Fig. 5), whatever the material structure (emulsion made of droplets with repulsive interactions, flocculated clay suspension, foam, or materials with more complex structures), the material concentration (for direct and inverse emulsions and clay suspension), and for various interactions between the interstitial liquid or the suspended elements and the solid surface (different surfactants in emulsions and different wetting properties of the interstitial liquid on the solid surface) [27].

This similar V_S vs τ_S variation along with the remarkable persistency of the value of δ, despite the physicochemical differences between all the materials and surfaces we tested, suggests that the origin of the wall slip for this range of systems lies at first order in their common property: a jammed structure filled with a mobile interstitial liquid. More precisely, any of the above jammed systems is made of elements of a size typically ranging in [0.1–10 μm]. The jammed structure they form is rough, with a roughness typically of the order of the element size, and, due to its yield stress, this structure shape is likely partly maintained at the approach of the smooth wall; i.e., in contrast with an unjammed material, the elements do not particularly align along the wall—they keep their 3D distribution, precisely because this is a jammed structure [see Fig. 1(b)]. The interstitial liquid fills the distance (d)

between the wall and the first element surface, and the displacement of the jammed structure as a block induces a flow of the liquid throughout this 3D porous structure. This is a Stokes flow requiring an average stress proportional to the velocity and liquid viscosity, via a single characteristic length δ reflecting this flow through a more or less complex structure roughly characterized by its porosity and pore size distribution. In our case, it happens that our samples with very different structure yield similar δ values. This might be due to the fact that highly squeezed structure (gels, emulsions, and microgels) have a large pore size but a low porosity, while a dispersed structure (clay) has a small pore size but a large porosity, two effects which more or less balance and could lead to similar resistance to liquid flow and thus similar apparent wall slip thickness. In this context, the second regime observed at the approach of τ_c (see Fig. 5) might simply be due to a progressively increasing erosion of the rough external jammed network exhibiting local stress resistances lower than τ_c.

This work has benefited from fruitful discussions with Michel Cloitre and from a French government grant managed by ANR within the frame of the national program *Investments for the Future* ANR-11-LABX-022-01 and ANR-10-EQPX-48-01.

[1] A. J. Liu and S. R. Nagel, Nature (London) **396**, 6706 (1998).
[2] H. A. Barnes, J. Non-Newtonian Fluid Mech. **56**, 221 (1995).
[3] S. Granick, Y. Zhu, and H. Lee, Nat. Mater. **2**, 221 (2003).
[4] M. Cloitre and R. T. Bonnecaze, Rheol. Acta **56**, 283 (2017).
[5] J. R. Stokes, M. W. Boehm, and S. K. Baier, Curr. Opin. Colloid Interface Sci. **18**, 349 (2013).
[6] S. Ozkan, T. W. Gillece, L. Senak, and D. J. Moore, Int. J. Cosmet. Sci. **34**, 193 (2012).
[7] L. Chen, Y. Duan, C. Zhao, and L. Yang, Chem. Eng. Process. **48**, 1241 (2009).
[8] T. T. Ngo, E. H. Kadri, R. Bennacer, and F. Cussigh, Constr. Build. Mater. **24**, 1253 (2010).
[9] N. Rungraeng, S. H. Yoon, Y. Li, and S. Jun, Trans. ASABE **58**, 861 (2015).
[10] G. Ovarlez, S. Rodts, X. Chateau, and P. Coussot, Rheol. Acta **48**, 831 (2009).
[11] J. Goyon, A. Colin, and L. Bocquet, Soft Matter **6**, 2668 (2010).
[12] U Yilmazer and D. M. Kalyon, J. Rheol. **33**, 1197 (1989); H. J. Walls, S. B. Caines, A. M. Sanchez, and S. A. Khan, J. Rheol. **47**, 847 (2003).
[13] P. Ballesta, R. Besseling, L. Isa, G. Petekidis, and W. C. K. Poon, Phys. Rev. Lett. **101**, 258301 (2008).
[14] P. Ballesta, G. Petekidis, L. Isa, W. C. K. Poon, and R. Besseling, J. Rheol. **56**, 1005 (2012).
[15] P. Ballesta, N. Koumakis, R. Besseling, W. C. K. Poon, and G. Petekidis, Soft Matter **9**, 3237 (2013).
[16] S. P. Meeker, R. T. Bonnecaze, and M. Cloitre, Phys. Rev. Lett. **92**, 198302 (2004).
[17] T. Divoux, V. Lapeyre, V. Ravaine, and S. Manneville, Phys. Rev. E **92**, 060301 (2015); S. Atkas, D. M. Kalyon, B. M. Marin-Santibanez, and J. Perez-Gonzalez, J. Rheol. **58**, 513 (2014); J. F. Ortega-Avila, J. Perez-Gonzalez, B. M. Marin-Santibanez, F. Rodriguez-Gonzalez, S. Atkas, M. Malik, and D. M. Kalyon, J. Rheol. **60**, 503 (2016).
[18] S. P. Meeker, R. T. Bonnecaze, and M. Cloitre, J. Rheol. **48**, 1295 (2004).
[19] J. B. Salmon, L. Becu, S. Manneville, and A. Colin, Eur. Phys. J. E **10**, 209 (2003).
[20] V. Bertola, F. Bertrand, H. Tabuteau, D. Bonn, and P. Coussot, J. Rheol. **47**, 1211 (2003).
[21] N. D. Denkov, S. Tcholakova, K. Golmeanov, K. A. Ananthpadmanabhan, and A. Lips, Soft Matter **5**, 3389 (2009).
[22] S. Marze, D. Langevin, and A. Saint-Jalmes, J. Rheol. **52**, 1091 (2008).
[23] N. D. Denkov, V. Subramanian, D. Gurovich, and A. Lips, Colloids Surf. A **263**, 129 (2005).
[24] N. D. Denkov, S. Tcholakova, K. Golemanov, V. Subramanian, and A. Lips, Colloids Surf. A **282**, 329 (2006).
[25] M. Le Merrer, R. Lespiat, R. Höhler, and S. Cohen-Addad, Soft Matter **11**, 368 (2015).
[26] P. Coussot, H. Tabuteau, X. Chateau, L. Tocquer, and G. Ovarlez, J. Rheol. **50**, 975 (2006).
[27] See Supplemental Material at http://link.aps.org/supplemental/10.1103/PhysRevLett.000.000000 for materials, surface characteristics, rheometry, and detailed results for the different materials.
[28] P. Coussot, Q. D. Nguyen, H. T. Huynh, and D. Bonn, Phys. Rev. Lett. **88**, 175501 (2002); J. Rheol. **46**, 573 (2002).
[29] J. R. Seth, M. Cloitre, and R. T. Bonnecaze, J. Rheol. **52**, 1241 (2008).
[30] R. D. Deegan, O. Bakajin, F. Dupont, G. Huber, S. R. Nagel, and T. A. Witten, Nature (London) **389**, 827 (1997).
[31] H. Van Damme, P. Levitz, J. J. Fripiat, J. F. Alcover, L. Gatineau, and F. Bergaya, in *Physics of Finely Divided Matter,* edited by N. Boccara and M. Daoud (Springer Verlag, Berlin, 1985), pp. 24–30.
[32] M. Morvan, D. Espinat, J. Lambard, and T. Zemb, Colloids Surf. A **82**, 193 (1994).
[33] J. M. Piau, J. Non-Newtonian Fluid Mech. **144**, 1 (2007).
[34] J. Boujlel, M. Maillard, A. Lindner, G. Ovarlez, X. Chateau, and P. Coussot, J. Rheol. **56**, 1083 (2012).